



Cite this: *Dalton Trans.*, 2015, **44**, 9370

Received 23rd March 2015,
Accepted 17th April 2015

DOI: 10.1039/c5dt01147g

www.rsc.org/dalton

Mixed-metal metallocavitands: a new approach to tune their electrostatic potentials for controllable selectivity towards substituted benzene derivatives†

Jian-Jun Liu,^a Ying-Fang Guan,^a Yong Chen,^a Mei-Jin Lin,^{*a,b} Chang-Cang Huang^{*a} and Wen-Xin Dai^a

We have successfully developed a new synthetic approach to modulate the electrostatic potentials of metallocavitands and thus their selective recognition towards substituted benzene derivatives via integrating two metal cations of different electronegativity into a self-assembled system.

Geometric and electronic complementarities are two fundamental characteristics for molecular recognition in supramolecular chemistry,¹ which refers to two interacting molecules complementing each other in shape, size and electrostatic potential, akin to the key and lock model postulated by Emil Fischer.² Utilizing such complementary effects, various applications including sensors, catalysis and separations have been developed in the past few decades.³ In order to improve the selectivity in these applications, the modulation of the shape and size effects is always the first choice.⁴ However, few examples focused on the electronic complementary effect.⁵ For investigating its origin, the electrostatic potentials of the cavity surfaces in most conventional organic hosts (*e.g.* cyclodextrins,⁶ cucurbiturils,⁷ calixarenes,⁸ cyclotrimeratrylenes⁹ and pillararenes¹⁰) are notoriously difficult to be tuned by organic syntheses.

Metallocavitands are an emerging class of hybrid hosts that combine organic and inorganic functional motifs,¹¹ which provides another possibility to regulate their electrostatic potentials by metal cations. To our surprise, a mixture of several different electronegative metal cations in inorganic materials is a common approach to tune their electrostatic potentials but remains less adopted in metal-organic hybrid

materials.¹² This may be due to most instances dominated by big organic motifs, and a limit contribution of metal cations to their electrostatic potentials.¹³ In theory, the above mixed-metal approach should be suitable for polynuclear metal-organic complexes because in such systems, metal ions are bridged by tiny amounts of organic atoms. Recently, we have reported a double-wall-hourglass shaped metallocavitand Zn_8L_8 bearing an aforementioned polynuclear cyclic core and an electron-deficient cavity, which exhibited an unusual selectivity towards substituted benzene derivatives (PhXs) of different electron densities during co-crystallizations.¹⁴ Herein, we report that the mixed-metal approach is indeed viable for our metallocavitands. The combination of multidentate acylthiosemicarbazide ligands **L** with a mixture of two different electronegativity Zn^{2+} and Cu^{2+} cations ($\chi = 1.6$ for Zn^{2+} and 1.9 for Cu^{2+})¹⁵ in different ratios leads to a series of mixed-metal metallocavitands $[Zn_{1-x}Cu_x]_8L_8$, whose cavity surfaces indeed possess adjustable electrostatic potentials. As a result, such metallocavitands exhibit a tunable selectivity towards substituted benzene derivatives during co-crystallizations. To the best of our knowledge, this is the first time that the electrostatic potentials of metallocavitands can be modulated by the mixed-metal approach has been reported.

As mentioned above, in the previous communication,¹⁴ we have already reported that the self-assembly of acylthiosemicarbazide ligands terminated by rigid benzoyl and flexible 2-(4-chlorophenoxy) acetyl moieties at both sides with equimolar amounts of zinc acetylacetonate in a mixture solvent of chloroform and *N,N*-dimethylacetamide (DMA) with a volume ratio of 1 : 1 at room temperature led to a colourless solution, followed by slow evaporation affording plate crystalline materials, which have been revealed to be a double-wall-hourglass shaped metallocavitand Zn_8L_8 ($M_1 = M_2 = Zn$ in Fig. 1) by single crystal structural analysis. Following the same synthetic process, however the replacement of zinc acetylacetonate with copper acetate afforded black block crystalline materials in a yield of 68%.

The single crystal X-ray diffraction analyses revealed that it is also an octanuclear metallocavitand (named as Cu_8L_8 ,

^aState Key Laboratory of Photocatalysis on Energy and Environment, College of Chemistry, Fuzhou University, China. E-mail: meijin_lin@fzu.edu.cn, cchuang@fzu.edu.cn; Tel: +0086 591 2286 6143

^bState Key Laboratory of Structural Chemistry, Fujian Institute of Research on the Structure of Matter, CAS, China

† Electronic supplementary information (ESI) available: Experimental details, crystallographic data, NMR, ICP, HRMS, and PXRD. CCDC 1021744–1021747. For ESI and crystallographic data in CIF or other electronic format see DOI: 10.1039/c5dt01147g

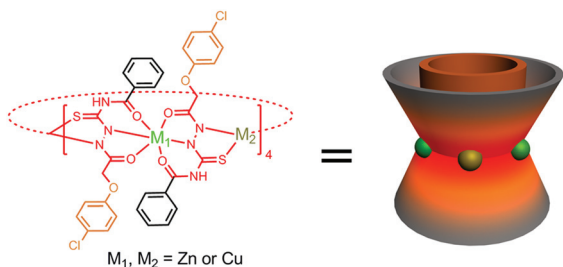


Fig. 1 Chemical structure (left) and schematic representation (right) of mixed-metal metallocavitands $[Zn_{1-x}Cu_x]_8L_8$.

Fig. 2). Similarly, the chelation of one six-coordinated copper cation by two perpendicular acylthiosemicarbazide ligand molecules leads to a dimeric complex through the formation of four Cu–O bonds (1.981–1.995 Å and 2.245–2.320 Å) between Cu^{2+} and two carbonyl oxygen atoms of each molecule together with two Cu–N bonds (1.939–1.992 Å) between Cu^{2+} and one deprotonated hydrazide nitrogen atom of each molecule, which is further interconnected by other four-coordinated copper cations through two Cu–S bonds (*ca.* 2.253 Å) and two Cu–N bonds (*ca.* 1.967 Å) to yield the final metallocavitand Cu_8L_8 . Due to a shorter metal ionic radius, the polynuclear core as well as the cavity center of the generated Cu_8L_8 (the distances of two opposite Cu^{2+} cations are around 12.43×13.35 Å) is slightly contracted compared to that of Zn_8L_8 (12.73×13.59 Å). Inside and outside of the cavity plenty of DMA solvent molecules are detected but most of them are largely disordered and could not be located in the crystal structure refinement. Therefore, all of the solvent contribution is subtracted from the data using SQUEEZE during the refinement.¹⁶

It is worthwhile pointing out that, compared with the crystal structure of Zn_8L_8 , a major difference in that of Cu_8L_8 is that its inner cavity is open and occupied by DMA molecules but not by the self-inclusive 4-chlorophenoxy group. The latter self-inclusion phenomenon was observed in the reported Zn_8L_8 , which somewhat reflected that the inner cavity was electron-deficient and it had a strong tendency towards electron-rich and geometrically appropriate guest molecules by elec-

tronic complementarity. Likewise, it seems that the inner cavity of Cu_8L_8 is not electron-deficient enough to trap a 4-chlorophenoxy group during the crystallization, which is supported by the theoretical calculations and selective co-crystallization experiments.

To make clear the difference between Cu_8L_8 and Zn_8L_8 , the Cu_8L_8 electrostatic potential was calculated by using its single-crystal structural data without any further optimizations. As shown in Fig. 3a, although the equatorial portions of Cu_8L_8 are electron-deficient (blue ring), the cavity surface is a little electron-rich (yellow maps in the centers), which is different from those in the self-inclusive Zn_8L_8 that showed an electron-deficient surface inside the cavity,¹⁴ which corroborates the results that self-inclusion of the 4-chlorophenoxy group was only observed in Zn_8L_8 but not in Cu_8L_8 . Considering the obvious difference between the self-inclusive structure of Zn_8L_8 and Cu_8L_8 , the electrostatic potential of an idealized zinc complex based on the structure of Cu_8L_8 by only replacing Cu^{2+} with Zn^{2+} without further optimizations (Zn_8L_8 bearing a similar open cavity to Cu_8L_8 , abbreviated as open Zn_8L_8) was also given for a parallel comparison (Fig. 3b). As expected, the latter presents a much more electron-deficient cavity surface than that of Cu_8L_8 . Thus, the metal cations indeed play a considerable role in the electrostatic potentials of our metallocavitands.

The close coordination behaviors of Zn^{2+} and Cu^{2+} cations in metallocavitands suggest that the structures of such M_8L_8 remained unchanged in a certain range when some of their metal cations are replaced by the second metals. That is, a series of isostructural metallocavitands are anticipated to be obtained by using a mixture of Zn^{2+} and Cu^{2+} cations in different molar ratios but not the pure one metal cation. However, this is of considerable significance for the modulation of their electron structures due to the obvious difference between the electrostatic potentials of Zn_8L_8 and Cu_8L_8 . Again, following the same synthetic process as Zn_8L_8 , but replacement of pure Zn^{2+} with a mixture of Zn^{2+} and Cu^{2+} cations in Cu^{2+} molar ratios of 5%, 10%, 15%, 20%, 25%, 30% and 35%

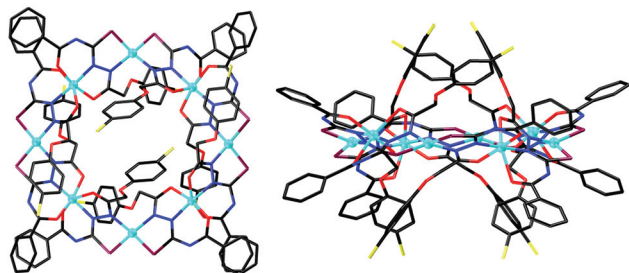


Fig. 2 Top (left) and side (right) views of the molecular structure of Cu_8L_8 in the crystal (aqua Cu, black C, red O, blue N, purple S, and yellow Cl). For clarity, all solvent molecules as well as hydrogen atoms were omitted.

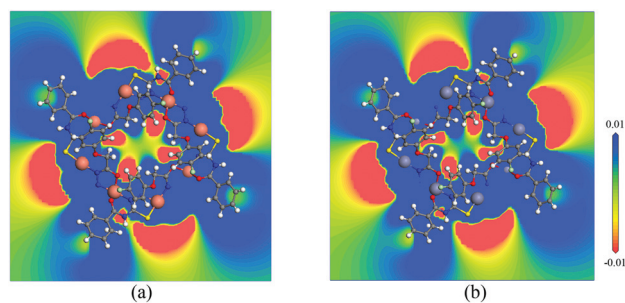


Fig. 3 The electrostatic potential surfaces plotted in cross-sections for Cu_8L_8 (a) and open Zn_8L_8 generated by replacing Cu in Cu_8L_8 with Zn (b). The electrostatic potential was in the full range at an isovalue of 0.001 electrons per Bohr³ for electron density and was visualized by a rainbow color ramp continuously from red–orange–yellow–green–cyan–blue (electron rich to electron poor).

resulted in 7 batches of black crystals $[\text{Zn}_{1-x}\text{Cu}_x]_8\text{L}_8$ ($x = 0.05, 0.10, 0.15, 0.20, 0.25, 0.30$ and 0.35).

Interestingly, although several potential structures exist, only one kind of crystal with the same colors and shapes was obtained in each batch. According to their appearances, 7 batches of black crystals can further be divided into two kinds of crystals: plate crystals for 5%–25%, and block crystals for 30% and 35%, which indeed are confirmed by powder X-ray diffraction (PXRD) analysis. As depicted in Fig. S11,[†] PXRD patterns of $[\text{Zn}_{1-x}\text{Cu}_x]_8\text{L}_8$ ($x = 0.05$ – 0.25) possess the same set of peaks as those of the recorded and simulated PXRD patterns of Zn_8L_8 , indicating that these 5 batches of crystals should be isostructural to that of the self-inclusive Zn_8L_8 , which is confirmed by the single crystal X-ray diffraction analyses. The latter revealed that the lattice parameters of these 5 batches of crystals are indeed totally the same (for details, see ESI[†]).

However, PXRD patterns of the left two batches of crystals are different from those of Zn_8L_8 . Despite they are very close to the simulated one of Cu_8L_8 , there are still some intense peaks that could not match each other. Accordingly, the structures of these two batches of crystals should have a very similar structural feature to those of Cu_8L_8 , which is also confirmed by single crystal structural analyses. As expected, the proof-of-the-concept example $[\text{Zn}_{1-x}\text{Cu}_x]_8\text{L}_8$ ($x = 0.35$) is an octanuclear metallocavitand with a little expanded cavity (the distances of two opposite metal cations are around $12.25 \times 14.00 \text{ \AA}$, Fig. 4), and all the 4-chlorophenoxy branches extend above and below the polynuclear macrocyclic core.

The accurate contents of two metal cations in each batch of as-synthesized crystals have been determined by inductively coupled plasma (ICP) atomic emission spectrometry, which revealed that all the recorded data are close to their theoretical values (Table S8, ESI[†]). For example, the weight percentage of Cu^{2+} in three crystalline samples $[\text{Zn}_{1-x}\text{Cu}_x]_8\text{L}_8$ ($x = 0.10, 0.25, 0.35$) are 9.44%, 24.44% and 38.75%, respectively, which can be calculated with formulae of $\text{Zn}_{7.22}\text{Cu}_{0.78}\text{L}_8$, $\text{Zn}_{6.00}\text{Cu}_{2.00}\text{L}_8$ and $\text{Zn}_{4.84}\text{Cu}_{3.16}\text{L}_8$, respectively.

Together with all the above evidence, two points can be drawn at present: (1) the use of a mixture of two metal cations in the self-assembly yields at least two kinds of metallocavi-

tands with very close configurations because the obtained crystals based on them are in one phase; (2) the distributions of the generated metallocavitand mixtures are dependent on the addition of two metal cation ratios during self-assembly. However, whether two metal cations are really mixed in the same metallocavitand molecules is still unclear. To clarify this question, the high-resolution mass spectra of Zn_8L_8 , $\text{Zn}_{7.22}\text{Cu}_{0.78}\text{L}_8$, $\text{Zn}_{6.00}\text{Cu}_{2.00}\text{L}_8$, $\text{Zn}_{4.84}\text{Cu}_{3.16}\text{L}_8$ and Cu_8L_8 have been recorded (Fig. S6–S10, ESI[†]). For Zn_8L_8 and Cu_8L_8 that are single components, the most abundant peaks were observed at $m/z = 3440.66$ and 3401.63 that show the characteristic m/z splitting for a positive species $[\text{Zn}_8\text{L}_8 + \text{Na}]^+$ of 1.03 mass units and a negative $[\text{Cu}_8\text{L}_8]^-$ of 0.997 mass units, respectively. Similarly, for $\text{Zn}_{7.22}\text{Cu}_{0.78}\text{L}_8$, $\text{Zn}_{6.00}\text{Cu}_{2.00}\text{L}_8$ and $\text{Zn}_{4.84}\text{Cu}_{3.16}\text{L}_8$, the most abundant peaks were detected at $m/z = 3415.67, 3413.63$ and 3411.61 , assigned to $[\text{Zn}_{7.22}\text{Cu}_{0.78}\text{L}_8]^+$, $[\text{Zn}_{6.00}\text{Cu}_{2.00}\text{L}_8]^-$ and $[\text{Zn}_{4.84}\text{Cu}_{3.16}\text{L}_8]^-$, respectively. Importantly, no molecular ion peaks of Cu_8L_8 and Zn_8L_8 were observed in $\text{Zn}_{7.22}\text{Cu}_{0.78}\text{L}_8$, $\text{Zn}_{6.00}\text{Cu}_{2.00}\text{L}_8$ and $\text{Zn}_{4.84}\text{Cu}_{3.16}\text{L}_8$, indicating that each of them is not a simple physical mixture of single-component copper and zinc metallocavitands, but more likely to be a mixture of at least two mixed-metal metallocavitands with two metal cations in one molecule.

From our previous experience on Zn_8L_8 and Cu_8L_8 , the electrostatic potentials of the cavity surfaces, as well as the selectivity towards PhXs during co-crystallizations for seven newly formed mixed-meal metallocavitands $[\text{Zn}_{1-x}\text{Cu}_x]_8\text{L}_8$ should fall in the range between those of the former two complexes. Due to the co-existence of several isomers for each mixed-meal metallocavitand, the calculation of their electrostatic potentials is rather difficult. Instead, the study of their selective co-crystallization behaviors that reflect the electrostatic potentials indirectly can be achieved. Following the reported process, co-crystallization of $[\text{Zn}_{1-x}\text{Cu}_x]_8\text{L}_8$ ($x = 0.05, 0.10, 0.15, 0.20, 0.25, 0.30$ and 0.35) with PhXs, including chlorobenzene (PhCl), bromobenzene (PhBr), iodobenzene (PhI), toluene (PhCH₃) and aniline (PhNH₂) in a solvent mixture of DMA, DMSO and chloroform (4 : 4 : 2 in volume) led to another 7 batches of black crystals. From their appearance, some interesting regulation can be found. There are only one kind of hexagonal crystal for all PhXs when $x = 0.05$, while there are plate crystals for PhCl, and hexagonal crystals for PhBr, PhI, PhCH₃ and PhNH₂ when $x = 0.10, 0.15$ and 0.20 . With increasing amounts of Cu^{2+} (more than 0.25), no hexagonal but only plate or block crystals are formed.

In our previous experience,¹⁴ plate crystals retain the structures of complexes $[\text{Zn}_{1-x}\text{Cu}_x]_8\text{L}_8$, while hexagonal crystals are their clathration of relevant PhXs, which indeed are confirmed by single-crystal X-ray diffraction and PXRD analyses. Thus, all PhXs can be trapped in a pure metallocavitand Zn_8L_8 during their co-crystallizations. With the addition of Cu^{2+} increasing, only the encapsulation contents of PhCl gradually reduce, and PhCl is totally excluded when the Cu^{2+} content is increased to around 10% (Fig. S1, ESI[†]). Subsequently, the inclusions of left four guests are also decreasing with the continually increasing Cu^{2+} , which is supported by the ¹H NMR spectral

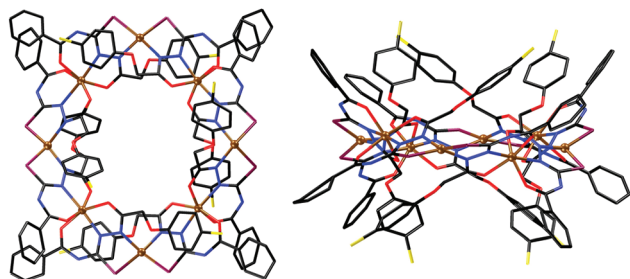


Fig. 4 Top (left) and side (right) views of the molecular structure of $[\text{Zn}_{1-x}\text{Cu}_x]_8\text{L}_8$ ($x = 0.35$) in the crystal (brown Cu or Zn, black C, red O, blue N, purple S, and yellow Cl). For clarity, all solvent molecules as well as hydrogen atoms were omitted.

study. The same amount of as-synthesized crystals $[Zn_{1-x}Cu_x]_8L_8$ ($x = 0.05, 0.10, 0.15, 0.20, 0.25, 0.30$) was obtained from PhBr by soaking in deuterated ethanol for 24 hours, the proton signal intensities around 7–8 ppm of released PhBr decrease gradually with the increasing Cu^{2+} ratios (Fig. S5, ESI†), which indicates that with the increase of the addition of Cu^{2+} cations, the encapsulated PhBr molecules decrease gradually. None of them can be co-crystallized in the mixed-metal $[Zn_{1-x}Cu_x]_8L_8$ when Cu^{2+} is more than 25%, which is supported by the 1H NMR spectral study (Fig. S2–S4, ESI†). Such a variety law indicates that with the increase of the addition of Cu^{2+} cations, the electrostatic potentials of cavity surfaces increase. According to the principle of electronic complementarity, the required electronic potentials of guest molecules increase correspondingly.

In summary, we have reported a simple but efficient approach to modulate the electron structures of metal–organic complexes. By using a mixture of two different electronegative metal cations in one self-assembly system, a series of mixed-metal metallocavitands with tunable electrostatic potentials have been formed, which exhibited an adjustable selectivity towards PhXs during co-crystallization. Although a mixed metal is widely known in metal–organic systems,¹⁷ this is the first time that the electrostatic potentials of metallocavitands can be modulated by such a mixed-metal approach has been reported. This successful experience provides a reference for spreading this simple but efficient approach to other metal–organic compounds.

We thank Prof. Xin Fang for her useful discussions. This work was supported by the National Natural Science Foundation of China (21202020), the Doctoral Fund of Ministry of Education of China (20123514120002), the Natural Science Foundation of Fujian Province (2014J01040 and 2014J01045), and the Science & Technical Development Foundation of Fuzhou University (2012-XQ-10 and 2013-XQ-14).

Notes and references

- (a) J.-M. Lehn, *Angew. Chem., Int. Ed.*, 1990, **29**, 1304; (b) B. Honig and A. Nicholls, *Science*, 1995, **268**, 1144; (c) N. Kishi, Z. Li, K. Yoza, M. Akita and M. Yoshizawa, *J. Am. Chem. Soc.*, 2011, **133**, 11438.
- E. Fischer, *Ber. Dtsch. Chem. Ges.*, 1894, **27**, 2985.
- (a) M. T. Reetz, *J. Am. Chem. Soc.*, 2013, **135**, 12480; (b) M. S. Masar III, N. C. Gianneschi, C. G. Oliveri, C. L. Stern, S. T. Nguyen and C. A. Mirkin, *J. Am. Chem. Soc.*, 2007, **129**, 10149; (c) R. Pinalli and E. Dalcanele, *Acc. Chem. Res.*, 2013, **46**, 399; (d) S. Zarra, D. M. Wood, D. A. Roberts and J. R. Nitschke, *Chem. Soc. Rev.*, 2015, **44**, 419; (e) K. Mulla, H. Shaik, D. W. Thompson and Y. Zhao, *Org. Lett.*, 2013, **15**, 4532; (f) J. Xue, Z. Jia, X. Jiang, Y. Wang, L. Chen, L. Zhou, P. He, X. Zhu and D. Yan, *Macromolecules*, 2006, **39**, 8905.
- (a) C.-F. Lee, D. A. Leigh, R. G. Pritchard, S. D. chultz, S. J. Teat, G. A. Timco and R. E. P. Winpenney, *Nature*, 2009, **458**, 314; (b) X. Chi, M. Xue, Y. Ma, X. Yan and F. Huang, *Chem. Commun.*, 2013, **49**, 8175; (c) T. Ogoshi, T. Akutsu, D. Yamafuji, T. Aoki and T. Yamagishi, *Angew. Chem., Int. Ed.*, 2013, **52**, 8111; (d) T. Nakamura, H. Ube and M. Shionoya, *Angew. Chem., Int. Ed.*, 2013, **52**, 12096; (e) J. R. Cochrane, A. Schmitt, U. Wille and C. A. Hutton, *Chem. Commun.*, 2013, **49**, 8504.
- (a) M. Juríček, J. C. Barnes, E. J. Dale, W.-G. Liu, N. L. Strutt, C. J. Bruns, N. A. Vermeulen, K. C. Ghooray, A. A. Sarjeant, C. L. Stern, Y. Y. Botros, W. A. Goddard III and J. F. Stoddart, *J. Am. Chem. Soc.*, 2013, **135**, 12736; (b) N. Kishi, M. Akita and M. Yoshizawa, *Angew. Chem., Int. Ed.*, 2014, **53**, 3604; (c) S. P. Black, A. R. Stefankiewicz, M. M. J. Smulders, D. Sattler, C. A. Schalley, J. R. Nitschke and J. K. M. Sanders, *Angew. Chem., Int. Ed.*, 2013, **52**, 5749.
- (a) J. Szejtli, *Chem. Rev.*, 1998, **98**, 1743; (b) F. Hapiot, S. Tilloy and E. Monflier, *Chem. Rev.*, 2006, **106**, 767; (c) L. X. Song, L. Bai, X. M. Xu, J. He and S. Z. Pan, *Coord. Chem. Rev.*, 2009, **253**, 1276; (d) C. O. Mellet, J. M. G. Fernández and J. M. Benito, *Chem. Soc. Rev.*, 2011, **40**, 1586; (e) D.-S. Guo and Y. Liu, *Acc. Chem. Res.*, 2014, **47**, 1925.
- (a) A. Day, R. J. Blanch, A. P. Arnold, S. Lorenzo, G. R. Lewis and I. Dance, *Angew. Chem., Int. Ed.*, 2002, **41**, 275; (b) J. Lagona, P. Mukhopadhyay, S. Chakrabarti and L. Isaacs, *Angew. Chem., Int. Ed.*, 2005, **44**, 4844; (c) K. Kim, N. Selvapalam, Y. H. Ko, K. M. Park, D. Kim and J. Kim, *Chem. Soc. Rev.*, 2007, **36**, 267; (d) A. C. Bhasikuttan, H. Pal and J. Mohanty, *Chem. Commun.*, 2011, **47**, 9959.
- (a) L. Baldini, A. Casnati, F. Sansone and R. Ungaro, *Chem. Soc. Rev.*, 2007, **36**, 254; (b) C. D. Gutsche, *Calixarenes: An Introduction*, Royal Society of Chemistry, Cambridge, U.K., 2nd edn, 2008; (c) L. Mutihac, J. H. Lee, J. S. Kim and J. Vicens, *Chem. Soc. Rev.*, 2011, **40**, 2777; (d) D.-S. Guo and Y. Liu, *Chem. Soc. Rev.*, 2012, **41**, 5907; (e) Y. Chen and Y. Liu, *Chem. Soc. Rev.*, 2010, **39**, 495.
- (a) A. Collet, *Tetrahedron*, 1987, **43**, 5725; (b) T. Brotin and J.-P. Dutasta, *Chem. Rev.*, 2009, **109**, 88; (c) M. J. Hardie, *Chem. Soc. Rev.*, 2010, **39**, 516; (d) M. J. Hardie, *Isr. J. Chem.*, 2011, **51**, 807.
- (a) H. Takemura, *Curr. Org. Chem.*, 2009, **13**, 1633; (b) M. Xue, Y. Yang, X. Chi, Z. Zhang and F. Huang, *Acc. Chem. Res.*, 2012, **45**, 1294; (c) Y.-W. Yang, Y.-L. Sun and N. Song, *Acc. Chem. Res.*, 2014, **47**, 1950.
- (a) A. M. Castilla, W. J. Ramsay and J. R. Nitschke, *Acc. Chem. Res.*, 2014, **47**, 2063; (b) R. Chakrabarty, P. S. Mukherjee and P. J. Stang, *Chem. Rev.*, 2011, **111**, 6810; (c) J. Jankolovits, C. M. Andolina, J. W. Kampf, K. N. Raymond and V. L. Pecoraro, *Angew. Chem., Int. Ed.*, 2011, **50**, 9660; (d) H. T. Chifotides and K. R. Dunbar, *Acc. Chem. Res.*, 2013, **46**, 894; (e) P. D. Frischmann and M. J. MacLachlan, *Chem. Soc. Rev.*, 2013, **42**, 871; (f) M. Yoshizawa, J. K. Klosterman and M. Fujita, *Angew. Chem., Int. Ed.*, 2009, **48**, 3418.
- (a) S. Ishida, M. Nakajima, T. Liang, K. Kihou, C.-H. Lee, A. Iyo, H. Eisaki, T. Kakeshita, Y. Tomioka, T. Ito and

- S. Uchida, *J. Am. Chem. Soc.*, 2013, **135**, 3158; (b) J.-C. Wu, J. Zheng, P. Wu and R. Xu, *J. Phys. Chem. C*, 2011, **115**, 5675; (c) W. Wei, Y. Dai and B. Huang, *J. Phys. Chem. C*, 2011, **115**, 18597; (d) S. George, S. Pokhrel, Z. Ji, B. L. Henderson, T. Xia, L. Li, J. I. Zink, A. E. Nel and L. Mädler, *J. Am. Chem. Soc.*, 2011, **133**, 11270; (e) K. Teshima, S. Lee, N. Shikine, T. Wakabayashi, K. Yubuta, T. Shishido and S. Oishi, *Cryst. Growth Des.*, 2011, **11**, 995.
- 13 (a) G. Li, W. Yu, J. Ni, T. Liu, Y. Liu, E. Sheng and Y. Cui, *Angew. Chem., Int. Ed.*, 2008, **47**, 1245; (b) J. L. Bolliger, A. M. Belenguer and J. R. Nitschke, *Angew. Chem., Int. Ed.*, 2013, **52**, 7958; (c) D. Fiedler, D. Pagliero, J. L. Brumaghim, R. G. Bergman and K. N. Raymond, *Inorg. Chem.*, 2004, **43**, 846.
- 14 (a) C.-C. Huang, J.-J. Liu, Y. Chen and M.-J. Lin, *Chem. Commun.*, 2013, **49**, 11512.
- 15 L. Pauling, *The Nature of the Chemical Bond and the Structure of Molecules and Crystals*, Cornell University Press, Ithaca, N.Y., 3rd edn, 1960, p. 93.
- 16 A. L. Spek, *Acta Crystallogr., Sect. D: Biol. Crystallogr.*, 2009, **65**, 148.
- 17 (a) Y.-B. Chen, Y. Kang and J. Zhang, *Chem. Commun.*, 2010, **46**, 3182; (b) Z.-Q. Jiang, G.-Y. Jiang, F. Wang, Z. Zhao and J. Zhang, *Chem. Commun.*, 2012, **48**, 3653.